This article has been accepted for publication in a future issue of this journal, but has not been fully edited. Content may change prior to final publication. Citation information: DOI 10.1109/TVT.2015.2445872, IEEE Transactions on Vehicular Technology

A Supervisory Control Algorithm for a Series Hybrid Vehicle with Multiple Energy Sources

Youngkwan Ko, Jeeho Lee and Hyeongcheol Lee *Member, IEEE*

***Abstract*— This paper presents a new power distribution strategy (PDS) for a series electric hybrid vehicle in the sense of minimizing fuel usage. The target vehicle has three energy sources, the engine and generator set, the battery, and the ultracapacitor; and two traction motors for front and rear wheels. Two step PDS based on the real-time optimization technique is proposed to distribute the demand power among three energy sources. Several existing PDSs, such as the thermostat strategy and power-follower strategy, are modified and applied to be compared with the proposed strategy. An optimal torque distribution strategy between front and rear traction motors is also proposed to minimize the electric energy consumptions and to further improve the fuel economy. Simulation results demonstrate the feasibility and effectiveness of the proposed strategies.**

***Index Terms*— Series Hybrid Electrical Vehicle (SHEV), Power Distribution Strategy, Equivalent Consumption Minimization Strategy (ECMS), Ultra-Capacitor, Optimal Torque Distribution**

I. Introduction

THE series hybrid electric vehicle (SHEV) has a mechanically decoupled structure of the engine from the driveline and uses the electric traction motor alone for traction. Therefore, the SHEV gives some advantages, such as the multi-gear transmission is not required and thus the engine can be operated at its maximum efficiency. On the other hand, the SHEV requires large-scale electric machines including a traction motor and a generator and compounds the inefficiencies of them [1]. Therefore, the SHEV has been researched and developed for large scale transportation systems such as buses, trucks [2], or military vehicle [3, 4, 5]

There are several different possibilities of configurations in the SHEV depending on the number of the traction motors and the ESS. Fig. 1 shows a target system which has two traction motor and gear combinations and the parallel connection of the battery and the ultracapacitor as the energy storage system (ESS). Therefore, in this configuration, three different energy sources (the engine and generator set (EGS), the battery, and the ultracapacitor) supply the electric energy to two traction motors. This configuration is especially suitable for off-road military vehicles which require four wheel drive ability and high instantaneous electrical power provided by the ultracapacitor for the special weapon systems.

Because the fuel usage limits the operation range, fuel economy is more important for the military hybrid electric vehicles (HEVs) than the other functions provided by HEVs. In general, the fuel economy of a HEV depends strongly on the implemented energy management strategy, which is the major part of the supervisory control [6, 7, 8]. The main goal of this paper is designing optimal power distribution strategy (PDS) which is real-time applicable for the target SHEV to minimize fuel usage.

Power distribution strategies among the energy sources of a HEV can be classified into largely two categories: the rule based strategy and the optimization based strategy. The rule based strategy, such as thermostat control [8, 9, 10, 11, 12], power follower control [13, 14], and fuzzy based control [15], is designed based on heuristics, intuition, human expertise, and even mathematical models and without a priori knowledge of a predefined driving cycle [8]. The rule-based strategy has been successfully used for commercial HEV. Thermostat (on–off) control strategy operates the EGS only on the optimal operating point (OOP) when the battery SOC is below certain level [8, 9, 10, 11, 12]. Power follower strategy operates the EGS on the locus of high efficiency points called optimal operating line (OOL) or within some efficient boundary [13, 14]. However, these strategies lack flexibility and robustness, and do not guarantee optimize the energy efficiency over the entire driving cycle. A fuzzy logic controller was used to make decisions for the power distribution between the EGS and battery to ensure that the vehicle operates in the low energy consumption and low emission condition [15]. A supervisory control strategy based on efficiency maximizing map which is generated by off-line calculation was proposed in [16]. The off-line calculation considers a power distribution ratio between the EGS and the battery; and the efficiency of each two energy sources. The rule-based strategy is effective in real-time energy management and appropriates to be practically implemented to the real production vehicles. However, this strategy does not guarantee the optimality of the fuel economy and emissions [6].

The linear quadratic regulation (LQR), one of the most popular optimal techniques, is applied for a military SHEV with a battery. The LQR controller achieved the control purposes such as maintaining a desired battery SOC level at the

Manuscript received July 14, 2011; revised December 31, 2014 and March 14, 2015; accepted May 4, 2015. This work was supported by the Technology Innovation Program (10047586, The source technology development of clean diesel-hybrid system for 1-liter car) funded By the Ministry of Trade, industry & Energy(MI, Korea) and the MSIP(Ministry of Science, ICT and Future Planning), Korea, under the C-ITRC(Convergence Information Technology Research Center) (IITP-2015-H8601-15-1005) supervised by the IITP(Institute for Information & communications Technology Promotion).

The authors are with the Department of Electrical Engineering, Hanyang University, Seoul 133-791, Korea (corresponding author: Hyeongcheol Lee, phone: 82-2-2220-1685; fax: 82-2-2220-4685; e-mail: hclee@hanyang.ac.kr).

This article has been accepted for publication in a future issue of this journal, but has not been fully edited. Content may change prior to final publication. Citation information: DOI 10.1109/TVT.2015.2445872, IEEE Transactions on Vehicular Technology

end of the mission, minimizing the power drawn from the engine, having the capability to supply electrical loads [17]. Stochastic optimal control is also applied to the SHEV. An optimal control policy is designed as a higher probability distribution to the states with low cost [18].

Because the global optimization strategy [8, 13, 19, 20] cannot be directly used for real-time energy management due to its non-causal property requiring knowledge of future power demands [6], the real-time optimization strategy is developed based on the instantaneous cost function.

Among the real-time optimization strategies, the equivalent consumption minimization strategy (ECMS) is a remarkable example of realization of Pontryagin's minimum principle for the real-time power management of the HEV. The ECMS uses the concept called the equivalent fuel consumption and explicitly formulates a cost function for the equivalent fuel consumption to be optimized, subject to constraints related charge sustainability, emissions reduction, and drivability [21]. An equivalence factor evaluating the fuel equivalence of electrical energy is defined variously in previous ECMS researches [11, 12, 21, 22]. Equivalent factor should be tuned depending on the information of future drive cycle [19, 20, 23]. The ECMS with combined cost map, which is calculated with fuel consumption map and multiple emission maps, is proposed in [24]. While the ECMS with a combined cost map improves optimization performance in the reduction of emissions and fuel consumption of the SHEV, this requires the whole drive cycle to be known in advance. To overcome this issue, the control rule is extracted from Pontryagin's Minimum Principal based optimal controller. The control rule shows that it does not require information of the whole drive cycle, but it requires only the cruise time and the amount of available regenerative energy during braking [25].

The ECMS typically causes frequent mode transitions [5] accompanied by engine start and stop, which is not acceptable because of the bad fuel economy, emissions, and drivability. However, little research has focused on preventing frequent mode transitions by the ECMS except in the case of raising the issue with a brief suggestion [22, 27].

Most previous research focused on the power distribution between the EGS and the battery. The use of the ultracapacitor can improve fuel economy as well as the battery life by mitigating the charge and discharge rate and reducing abrupt current flows. Only a few research projects have been performed on the PDS including the ultracapacitor in the SHEV. A simple control strategy, in which the ultracapacitor supplies the high frequency parts of the demand power to extend the battery life, has been researched [14, 21]. However, since this strategy lacked of the state of charge (SOC) management, the ultracapacitor is often unavailable at low SOC. Moreover, this strategy did not provide real-time optimization of the PDS in the sense of minimization of fuel usage.

This paper presents a new PDS for a military SHEV shown in Fig. 1 in the sense of minimizing fuel usage. Two step PDS based on the real-time optimization technique is proposed to distribute the demand power among three energy sources. In the first step, the power distribution in the energy storage system (i.e., between the battery and the ultracapacitor) is conducted by minimizing a cost function consisting of instantaneous power consumptions of the battery and the ultracapacitor. The power distribution between the ESS and the EGS is accomplished in the second step by applying the modified ECMS. Several existing PDSs, such as the thermostat strategy and power-follower strategy, are modified and applied to be compared with the proposed strategy. The optimal torque distribution strategy between front and rear traction motors is also proposed to minimize the electric energy consumptions and to further improve the fuel economy. Simulation results demonstrate the feasibility and effectiveness of the proposed strategies.

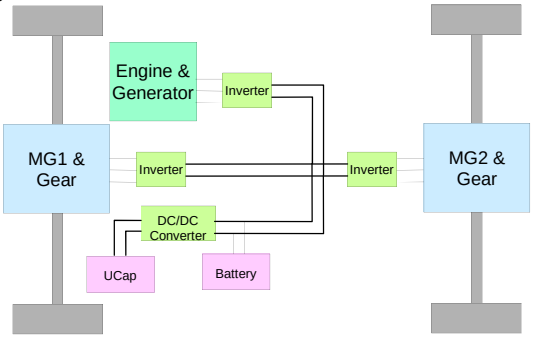

Fig. 1 Configuration of the target SHEV

II. System Description

A. System Configuration

As shown in Fig. 1, the target SHEV which is designed for off-road military vehicles has two traction motor and gear combinations and the parallel connection of the battery and the ultracapacitor as the ESS. The four wheel drive feature by installing two traction motor and gear combinations to the front and rear wheels can improve the traction performance of the vehicle on off-roads. The ultracapacitor with high specific power can support high instantaneous electrical power demand for special weapon systems.

As shown in Table I, a lithium based battery has good specific energy while an ultracapacitor has superior specific power [14, 21]. Therefore, the effective hybridization of a battery with an ultracapacitor can maximize the performance of the ESS by preserving the advantages of both the battery and the ultracapacitor. For example, the hybridization of the ESS can achieve high specific energy by the battery and high specific power by the ultracapacitor at the same time; and can extend the battery life by mitigating the charge and discharge rate and reducing abrupt current flows.

TABLE I
CHARACTRIETECS OF THE BATTERY AND THE ULTRACAPACITOR

Properties	Battery	Ultracapacitor
Specific Energy (storage)	10 ~ 100 Wh/Kg	5 ~ 10 Wh/Kg
Specific Power (delivery)	< 1,000 W/Kg	< 10,000 W/Kg
Charge/Discharge Efficiency	50~85%	85%~98%
Cycle Life (100% DOD)	1,000	> 500,000

A DC/DC converter is installed between the battery and the ultracapacitor to actively control the power flow between the battery and the ultracapacitor and to fully use the energy in the ultracapacitor. Therefore, the power distribution between the battery and the ultracapacitor can be actively controlled by

This article has been accepted for publication in a future issue of this journal, but has not been fully edited. Content may change prior to final publication. Citation information: DOI 10.1109/TVT.2015.2445872, IEEE Transactions on Vehicular Technology

controlling the DC/DC converter. The power distribution between the ESS and the EGS can be further controlled by the engine power management. This paper focuses on the power distribution ratios between three energy sources and does not confront how to control the DC/DC converter or how to manage the engine power to realize the power distribution ratios [21]. The specification of the target vehicle is determined based on the required performance as shown in Table II.

TABLE II
SPECIFICATION OF THE TARGET SHEV

Component	Parameter	Value	Units
Vehicle	Mass	5000	Kg
Engine	Type	Diesel	-
	Rated power	171	kW
Generator	Peak power	140	kW
Battery	Voltage	700	V
	Peak power	140	kW
	Rated power	80	kW
	Capacity	17.5	Ah
Ultra Capacitor	Peak power	180	kW
	Capacity	10	F
	Internal Resistance	0.144	Ohm
MG1	Peak power	96.18	kW
	Rated power	47.20	kW
MG2	Peak power	145.31	kW
	Rated power	71.31	kW

B. Energy Storage System Modeling

The internal resistance and the voltage curve with respect to the state of the charge (SOC) of the battery are given in Fig. 2 and 3. A mathematical model of the ESS is necessary to design the PDS based on the real-time optimization technique. Fig. 4 shows a simplified circuit of the ESS.

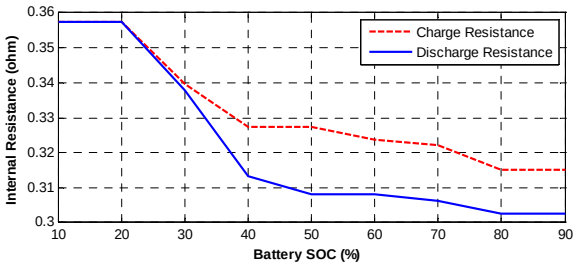

Fig. 2 Battery internal resistance according to battery SOC

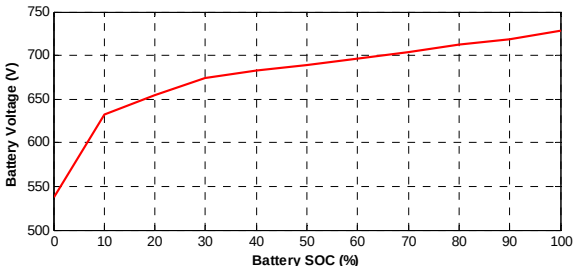

Fig. 3 Battery open circuit voltage according to Battery SOC

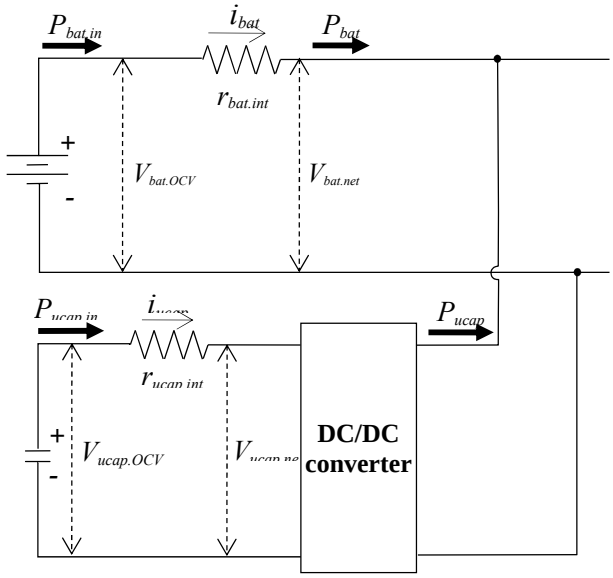

Fig. 4 Simplified circuit of the ESS

From Fig. 4, the consumed electric power by the battery and the ultracapacitor can be calculated as

$$P_{bat.in} = P_{bat.} + r_{bat.int} \times i_{bat}^{\ 2} \tag{1}$$

$$P_{ucap.in} = \begin{cases} \dfrac{P_{ucap}}{\eta_{dc.con}} + r_{ucap.int} i_{ucap}^{\ 2} & when \ \ i_{ucap} \geq 0 \\ P_{ucap}\eta_{dc.con} + r_{ucap.int} i_{ucap}^{\ 2} & when \ \ i_{ucap} < 0 \end{cases} \tag{2}$$

where $r_{bat.int}$ and $r_{ucap.int}$ are the internal resistance, i_{bat} and i_{ucap} are the currents through the battery and the ultracapacitor, $\eta_{dc.con}$ is the efficient of the DC/DC converter, and $P_{bat.in}$ and $P_{ucap.in}$ are the actual output power of the battery and the ultracapacitor to supply the demand power P_{bat} and P_{ucap} to the bus. The current i_{bat} and i_{ucap} can be obtained from

$$\begin{aligned} &P_{bat} = V_{bat.net} \cdot i_{bat} = (V_{bat.OCV} - r_{bat.int} \cdot i_{bat}) \cdot i_{bat} \\ &\therefore \ i_{bat} = \frac{V_{bat.OCV} - \sqrt{V_{bat.OCV}^{\ 2} - 4 \cdot P_{bat} \cdot r_{bat.int}}}{2 \cdot r_{bat.int}} \end{aligned} \tag{3}$$

$$\begin{aligned} &P_{ucap} = V_{ucap.net} i_{ucap} \eta_{dc.con} = (V_{ucap.OCV} - r_{ucap.int} i_{ucap}) \cdot i_{ucap} \eta_{dc.con} \\ &\therefore i_{ucap} = \frac{V_{ucap.OCV} - \sqrt{V_{ucap.OCV}^{\ 2} - 4(P_{ucap} / \eta_{dc.con}) \cdot r_{ucap.int}}}{2 r_{ucap.int}} \quad when \ \ i_{ucap} \geq 0 \\ &P_{ucap} = \frac{V_{ucap.net} i_{ucap}}{\eta_{dc.con}} = \frac{(V_{ucap.OCV} - r_{ucap.int} i_{ucap}) \cdot i_{ucap}}{\eta_{dc.con}} \\ &\therefore i_{ucap} = \frac{V_{ucap.OCV} - \sqrt{V_{ucap.OCV}^{\ 2} - 4 P_{ucap} \eta_{dc.con} r_{ucap.int}}}{2 r_{ucap.int}} \quad when \ \ i_{ucap} < 0 \end{aligned} \tag{4}$$

III. SUPERVISORY CONTROL

A. Optimal Torque Distribution

The target HEV has two different traction motors to drive the front and rear wheels. Because the efficiency of the motors depends on the angular velocity and the output torque of the motors, the necessary electric power to conduct the requested maneuver depends on the torque distributions between two

This article has been accepted for publication in a future issue of this journal, but has not been fully edited. Content may change prior to final publication. Citation information: DOI 10.1109/TVT.2015.2445872, IEEE Transactions on Vehicular Technology

motors. The optimal torque distribution which minimizes the necessary electric power can be obtained by solving an instantaneous optimization problem. If the instantaneous cost function is defined by the total power of two motors,

$$J_{motor} = P_{mf}(T_{mf}, \omega_{mf}) + P_{mr}(T_{mr}, \omega_{mr}) \tag{5}$$

where P_{mf} and P_{mr} are the motor powers, T_{mf} and T_{mr} are the motor output torques, and ω_{mf} and ω_{mr} are the motor angular velocities, the optimal torque distribution can be obtained by minimizing the instantaneous cost function.

$$\begin{aligned}\min_{T_{mf},T_{mr}} J_{motor} &= \min_{T_{mf},T_{mr}} \left[P_{mf}(T_{mf}, \omega_{mf}) + P_{mr}(T_{mr}, \omega_{mr})\right] \\ &= \min_{T_{mf},T_{mr}} \left[\frac{T_{mf}\omega_{mf}}{\eta_{mf}(T_{mf}, \omega_{mf})} + \frac{T_{mr}\omega_{mr}}{\eta_{mr}(T_{mr}, \omega_{mr})}\right]\end{aligned} \tag{6}$$

This cost function is subject to

$$\begin{aligned}&\omega_{mf} = g_f \frac{v_x}{r_w}, \quad \omega_{mr} = g_r \frac{v_x}{r_w} \\ &T_{des} = g_f T_{mf} + g_r T_{mr} \\ &T_{mf.gen\max} \le T_{mf} \le T_{mf.mot\max} \\ &T_{mr.gen\max} \le T_{mr} \le T_{mr.mot\max}\end{aligned} \tag{7}$$

where g_f and g_r are the gear ratios between the motors and the front and rear wheels, v_x is the vehicle longitudinal velocity, r_w is the wheel radius, $T_{mf.gen\_max}$, $T_{mf.mot\_max}$, $T_{mr.gen\_max}$ and $T_{mr.mot\_max}$ are the maximum regeneration and traction torque of the front and rear motors, and T_{des} is the desired total torque to perform the requested maneuver by the driver. The optimal front and rear torques can be calculated by scanning the torque, which minimizes the cost function (5) for the given desired torque and the vehicle velocity during the control loop time. As shown in Fig. 5, if the traction control or the stability control of the vehicle is necessary in a certain circumstance, the torque distribution to minimize electric energy is overridden by the vehicle dynamics control, which is not considered in this paper.

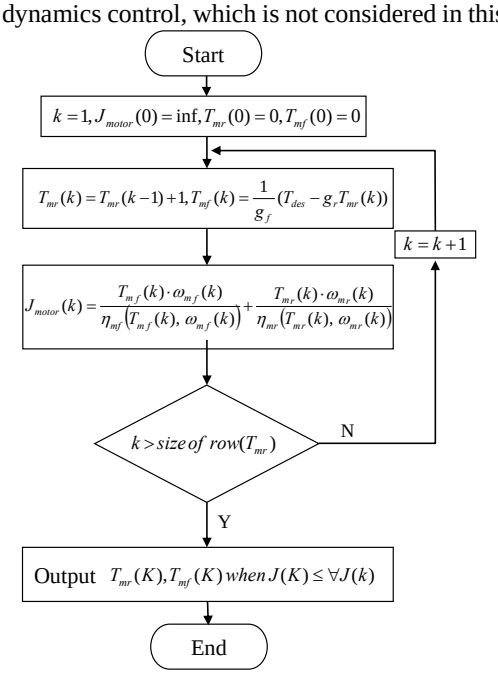

Fig. 5 Flowchart of optimal torque distribution algorithm

B. Power Distribution

The target system of this paper has three different energy sources. The power management strategy was not studied for this type of energy supply system for a SHEV so far. This paper proposes several different power management strategies among the energy sources by modifying the conventional strategies. Especially, this paper presents a modified thermostat control, a modified power follower control, and a modified ECMS.

1) Thermostat Control Strategy

Thermostat control strategy (TCS) controls the EGS operation by the ESS SOC. When the SOC of the ESS reaches its preset top line, the engine/generator is turned off and the vehicle is propelled only by the ESS. On the other hand, when the SOC of the ESS reaches its bottom line, the EGS is turned on and operated at its optimal operating point (OOP), and charges the ESS [23]. Since the ultracapacitor as well as the battery are used as the ESS in order to reduce the abrupt battery power changes and to extend the battery life, the conventional TCSs [9] which use only the battery cannot be directly applied in this research. A modified TCS for the target system is derived as follows.

If the on–off state of the EGS is indicated by R_{egs} (i.e., R_{egs} =1 implies the EGS on and R_{egs} =0 implies the EGS off), the power distribution among three energy sources can be obtained as

$$\begin{aligned}&P_{egs} = \begin{cases} P_{OOP} & when\ \ R_{egs}=1 \\ 0 & when\ \ R_{egs}=0 \end{cases} \\ &P_{bat} = LPF(P_{des} - P_{egs}) + P_{ucap.SOC} \\ &P_{ucap} = P_{des} - P_{egs} - P_{bat} - P_{ucap.SOC}\end{aligned} \tag{8}$$

where P_{egs} is the EGS power, P_{OOP} is the EGS power at the optimal operating point, P_{bat} is the battery power, P_{ucap} is the ultracapacitor power, $P_{ucap.SOC}$ is the ultracapacitor compensation power. A low pass filter (LPF) is used to assign the low frequency part of the ESS demand power to the battery and the high frequency part to the ultracapacitor. The ultracapacitor compensation power is the electric power to compensate ultracapacitor by the difference between present and target SOCs of the ultracapacitor and, in this paper, can be calculated by

$$\begin{aligned}&P_{ucap.SOC} = P_{ucap.comp} \cdot k_{ucap.SOC} \cdot k_{APS} \\ &k_{ucap.SOC} = SOC_{ucap.tar}(v_x) - SOC_{ucap} \\ &k_{APS} = \begin{cases} \exp(-\beta \cdot \frac{dx_{ap}}{dt}) & when\ \ \frac{dx_{ap}}{dt} \ge 0 \\ 1 & when\ \ \frac{dx_{ap}}{dt} < 0 \end{cases}\end{aligned} \tag{9}$$

where $P_{ucap.comp}$ is the compensation power parameter of the ultracapacitor, x_{ap} is the accelerator pedal displacement, $k_{ucap.SOC}$ is the difference between the present SOC (SOC_{ucap}) and the velocity dependent target SOC ($SOC_{ucap.tar}(v_x)$) of the ultracapacitor.

If current vehicle velocity is high and therefore more likely to

This article has been accepted for publication in a future issue of this journal, but has not been fully edited. Content may change prior to final publication. Citation information: DOI 10.1109/TVT.2015.2445872, IEEE Transactions on Vehicular Technology

be lowered in near future, it is better to reduce the ultracapacitor SOC level at low value to increase the regeneration amount during deceleration. On the other hand, if the vehicle velocity is low and so is more likely to be higher, it is better to increase and keep the SOC level of the ultracapacitor at high value to provide high demand power for acceleration. Therefore, the SOC of the ultracapacitor should be controlled such that the ultracapacitor SOC is maintained at high level by setting $SOC_{ucap.tar}(v_x)$ to be high value at low vehicle velocity and is maintained at low level with low $SOC_{ucap.tar}(v_x)$ value at high velocity. In this paper, the SOC of the ultracapacitor can be controlled based on the vehicle velocity by the velocity depending $SOC_{ucap.tar}(v_x)$ as shown in Fig.6 and equation (9).

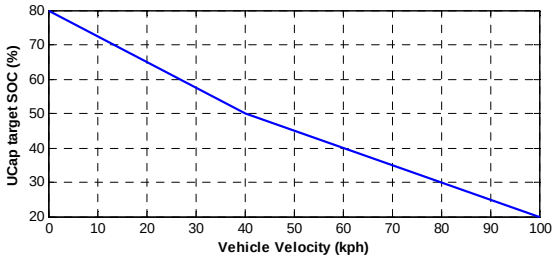

The function k_{APS} is used to reduce the compensation power of the ultracapacitor and to output more electric power when the driver presses the accelerator pedal. The parameter β in equation (9) is a tuning factor to adjust k_{APS} according to accelerator pedal change rate. The compensation power of the ultracapacitor is decreased by increasing β because k_{APS} is decreased even with the same accelerator pedal input.

Table III shows the operation condition of the EGS depending on the battery SOC. In this table, $SOC_{bat.lower}$ and $SOC_{bat.upper}$ are the lower and upper bounds of the battery. The TCS is simple and easy to design and apply to the real system. However, the TCS uses the battery so often and so wide SOC range that it may shorten battery life and worsen battery efficiency.

TABLE III
Operation condition of the EGS in TCS

Previous EGS State	ESS States	EGS State
ON	$SOC_{bat.upper} \geq SOC_{bat}$	ON
	$SOC_{bat.upper} < SOC_{bat}$	OFF
OFF	$SOC_{bat.lower} \geq SOC_{bat}$ or $P_{des} \geq (P_{bat.\max} + P_{ucap.\max})$	ON
	$SOC_{bat.lower} < SOC_{bat}$ and $P_{des} < (P_{bat.\max} + P_{ucap.\max})$	OFF

2) Power-Follower

The Power-follower control strategy (PCS) also controls the operation of the EGS by the SOC of the ESS. While the TCS controls the EGS in on-off manner, the PCS controls the EGS to provide a variable power depending on the battery SOC. Therefore, by the PCS, the EGS is active under almost all driving conditions, except for those conditions when low driving power is required and the SOC is greater than upper SOC limit. The PCS can reduce the battery usage and SOC range so that the battery life is extended and the battery efficiency is improved. Since the ultracapacitor is additionally installed in the ESS in this research, conventional PCSs should be modified.

In this research, conventional PCSs cannot be directly applied because the ultracapacitor is additionally used. The conventional PCSs considered driver demand power and battery SOC compensation power in determining the EGS power. The modified PCS distributes driver demand power to each energy sources (the EGS, the battery, and the ultracapacitor) while restraining fluctuations of the EGS operating point and excluding high frequency components from the battery power.

The modified PCS is divided into following 3 control steps according to the EGS power modification. In the first step, the EGS power is determined both to satisfy the driver's demand power and sustain the battery and ultracapacitor SOC in an appropriate level. The EGS power at the first step is determined as equation (10).

$$\begin{aligned} P_{egs1} &= P_{des} + P_{bat.SOC} + P_{ucap.SOC} \\ P_{bat.SOC} &= P_{bat.comp} \cdot k_{bat.SOC} \\ k_{bat.SOC} &= \frac{(SOC_{bat.upper} + SOC_{bat.lower})/2 - SOC_{bat}}{(SOC_{bat.upper} - SOC_{bat.lower})} \end{aligned} \quad (10)$$

where P_{egs1} is the temporary EGS power which will be replaced in the second and third step, $P_{ucap.SOC}$ is the ultracapacitor SOC compensation power, $P_{bat.SOC}$ is the battery SOC compensation power.

The battery SOC compensation power is calculated as the product of battery charge power constant term ($P_{bat.comp}$) and SOC error term ($k_{bat.SOC}$) between current and target SOCs.

In the second step, an engine on/off state is determined and the EGS power command determined in the first step is restricted within high fuel efficiency region between $P_{min.OOL}$ and $P_{max.OOL}$ which are on the OOL (Optimal Operating Line). Table IV and equation (11) shows these operations.

TABLE IV
Operation condition of the EGS in PCS

Previous EGS State	ESS States	EGS State
ON	$SOC_{bat} < SOC_{bat.upper}$ and $P_{egs1} < P_{eng.off}$	ON
	$SOC_{bat} > SOC_{bat.upper}$ or $P_{egs1} \geq P_{eng.off}$	OFF
OFF	$\left\{ SOC_{bat} < SOC_{bat.lower} \text{ or } P_{des} > P_{\max.dischg} \text{ or } P_{egs1} < P_{\max.OOL} \right\}$ and $P_{egs1} < P_{eng.of}\, f$	ON
	$SOC_{bat} > SOC_{bat.lower}$	OFF

$$P_{egs2} = \begin{cases} P_{\min.OOL} & when \;\; P_{egs1} < P_{\min.OOL} \text{ and } R_{egs} = 1 \\ P_{egs1} & when \;\; P_{\min.OOL} \leq P_{egs1} \leq P_{\max.OOL} \text{ and } R_{egs} = 1 \\ P_{\max.OOL} & when \;\; P_{egs1} > P_{\max.OOL} \text{ and } R_{egs} = 1 \\ 0 & when \;\; R_{egs} = 0 \end{cases} \quad (11)$$

As shown in Table IV, the proposed PCS determines the on/off operation of the EGS, using not only the P_{egs1} but also the battery SOC. $P_{eng.off}$ is the maximum value of the ESG

This article has been accepted for publication in a future issue of this journal, but has not been fully edited. Content may change prior to final publication. Citation information: DOI 10.1109/TVT.2015.2445872, IEEE Transactions on Vehicular Technology

operation used to protect the battery from over-charge caused by massive EGS charging power. $P_{max.OOL}$ is a limit value to protect the battery from over-discharge.

In the last step, the EGS power command is finally determined to prevent a rapid change of the EGS operating point. There are two parameters used to set the final EGS power command. One of the two parameters is the least keeping time (T_a) which makes the EGS maintain the operating point for a certain period of time. The other one is the least EGS power variation threshold (P_{delta}).

The EGS power command could be changed only when the difference between the EGS power command at the current time step and the one at the previous time step is bigger than P_{delta}. While P_{egs} stays constant, $P_{egs2.ave}$ is an average value of P_{egs2} during the least keeping time. After the least keeping time, if the difference between the average EGS power command $P_{egs2.ave}$ and the previous EGS power command ($P_{egs}(t\text{-}T_a)$) is higher than the least EGS power variation P_{delta}, P_{egs} will be changed into $P_{egs2.ave}$. Otherwise, P_{egs} will not be changed for the next keeping time.

As shown in Fig.7, the least keeping time T_a is a function of the absolute value of $k_{bat.SOC}$ defined in equation (10). The high absolute value of $k_{bat.SOC}$ means the current battery SOC is far away from the target SOC. In this case, T_a will be small value to update P_{egs} and be able to sustain the battery SOC. On the other hand, the low absolute value of $k_{bat.SOC}$ makes T_a bigger and P_{egs} will be updated slowly.

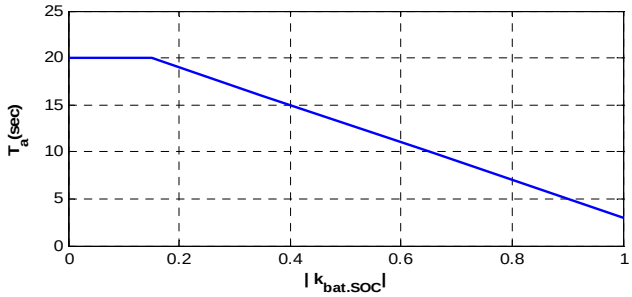

Fig. 7 T_a according to $k_{bat.SOC}$

As shown in Fig. 8, P_{delta} is a function of P_{egs2}. If P_{egs2} is close to OOP, P_{delta} will be a large value so that it is hard to update P_{egs} with such a little change of P_{egs2}. On the other hand, if P_{egs2} is far away from OOP, P_{delta} will be a small value that makes it easy to change P_{egs} into a new EGS power command $P_{egs2.ave}$. This feature makes the EGS operate frequently nearby the OOP to increase a fuel economy. As shown in equation (12), the proposed PCS distributed demand power to the EGS, battery and ultracapacitor.

$$P_{egs2.ave} = \int_{t}^{t+T_a} P_{egs2}\, dt$$

$$P_{egs} = \begin{cases} P_{egs2.ave}(t) & when, \left|P_{egs2.ave}(t) - P_{egs}(t-T_a)\right| > P_{delta} \text{ and } S_{egs} = 1 \\ P_{egs}(t-T_a) & when, \left|P_{egs2.ave}(t) - P_{egs}(t-T_a)\right| < P_{delta} \text{ and } S_{egs} = 1 \\ 0 & when,\ S_{egs} = 0 \end{cases} \quad (12)$$

$$P_{bat} = LPF(P_{des} - P_{egs}) + P_{ucap\_SOC}$$

$$P_{ucap} = P_{des} - P_{egs} - P_{bat} - P_{ucap\_SOC}$$

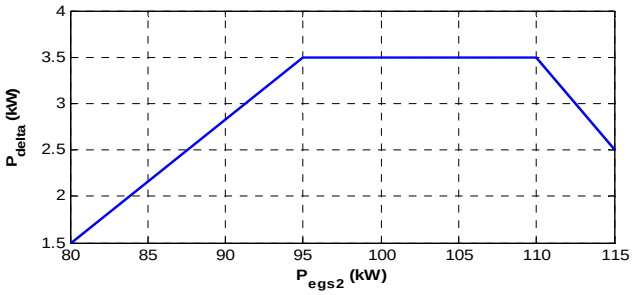

Fig. 8 P_{delta} according to P_{egs2}

3) ECMS

The previous research on the ECMS of a SHEV focuses on the power distribution between the EGS and the battery. The ECMS proposed in this paper is the real-time optimization strategy considering three energy sources: the engine and generator set, the battery, and the ultracapacitor. In the ECMS, the power distribution for the energy sources for obtaining driving power of the vehicle is achieved in the sense of minimizing fuel usage. The battery and ultracapacitor provide electrical energy to the driving motors without fuel usage, but the electrical energy stored in the battery and ultracapacitor should be produced by converting mechanical energy generated by the engine. Therefore, the equivalence factor evaluating the fuel equivalence of electrical energy can be evaluated by considering energy flow on the powertrain. The ECMS explicitly formulates a cost function for the equivalent fuel consumption to be optimized and determines optimal power distribution for the three energy sources.

Two step power distribution strategy (PDS) based on the real-time optimization technique is proposed to distribute the demand power among three energy sources. In the first step, the power distribution in the energy storage system (i.e., between the battery and the ultracapacitor) is conducted by minimizing a cost function consisting of instantaneous power consumptions of the battery and the ultracapacitor. In order to solve the optimal problem finding the power distribution ratio among the EGS and the ESS, power distribution ratio $u_1 = P_{bat}/P_{ESS}$ between the battery and the ultracapacitor is computed in advance by varying EGS demand power. At this step, characteristics of the battery and the ultracapacitor is considered in determining the power distribution ratio u_1. The instantaneous cost function including battery and ultracapacitor power is shown in equation (13).

At first, the EGS demand power P_{egs} is varied from 0 to $P_{egs.max}$ and accordingly the ESS demand powers are computed as ($P_{des} - P_{egs}$) to satisfy driver's desired power P_{des}. At each ESS demand power P_{ESS}, the optimal power distribution ratio u_1^* is computed by varying u_1 from $P_{bat.maxChg}/P_{ESS}$ to $P_{bat.maxDis}/P_{ESS}$. This first step results in 1 dimensional optimal map as a function of EGS demand power $u_1^* = f^*(P_{egs})$, calculated from

$$\min_{u_1} J_{ESS}(n) = \min_{u_1} \{ P_{bat.in}(P_{bat}(n)) + \alpha \left\| P_{bat}(n) - P_{bat}(n-1) \right\| + S_{ucap} P_{ucap.in}(P_{ucap}(n)) \} \quad (13)$$

where $u_1 = P_{bat}/P_{ESS} = f(P_{egs})$ which is subjected to $P_{ESS} =$

This article has been accepted for publication in a future issue of this journal, but has not been fully edited. Content may change prior to final publication. Citation information: DOI 10.1109/TVT.2015.2445872, IEEE Transactions on Vehicular Technology

$P_{des} - P_{egs} = P_{bat} + P_{ucap}$, $0 \le P_{egs} \le P_{egs.max}$, $P_{bat.maxChg} \le P_{bat} \le P_{bat.maxDis}$, $P_{ucap.maxChg} \le P_{ucap} \le P_{ucap.maxDis}$ and $SOC_{bat.lower} \le SOC_{bat} \le SOC_{bat.upper}$.

In equation (13), the inputs powers of the ESS $P_{bat.in}$ and $P_{ucap.in}$ are calculated by the electrical models presented in equations (1) to (4) which only represent static properties of the battery and the ultracapacitor. In the ECMS, the dynamic models are difficult to consider in calculating the instantaneous cost since the ECMS should be implemented in real-time. However, as shown in table I, the dynamic characteristics of the battery and the ultracapacitor are very different and its consideration in the ECMS can improve fuel economy as well as the battery life. Therefore, the proposed ECMS includes a change rate of the battery power $\alpha \| P_{bat}(n) - P_{bat}(n-1) \|$ in the instantaneous cost function. This additional term can mitigate the charge and discharge rate of the battery and, thereby, reduce abrupt battery current by applying low-pass filter property to the ECMS. The α in the additional term plays a role like time constant of the low-pass filter. If α is increased, change rate of the battery power is more weighted in the cost function and there are little changes on the obtained battery demand power. In equation (13), S_{ucap} is a charge sustaining factor of the ultracapacitor. Since $k_{ucap.SOC} = SOC_{ucap.tar}(v_x) - SOC_{ucap}$ from equation (9), if the ultracapacitor SOC is lower than the target SOC, S_{ucap} should be large to apply a penalty on the cost function. On the other hand, if the ultracapacitor SOC is higher than the target SOC, S_{ucap} should be small to reduce a penalty. Therefore, the S_{ucap} curve can be defined as shown in Fig. 9. The demand power of the ultracapacitor is weighted according to the S_{ucap} in order to sustain the ultracapacitor SOC within an appropriate level.

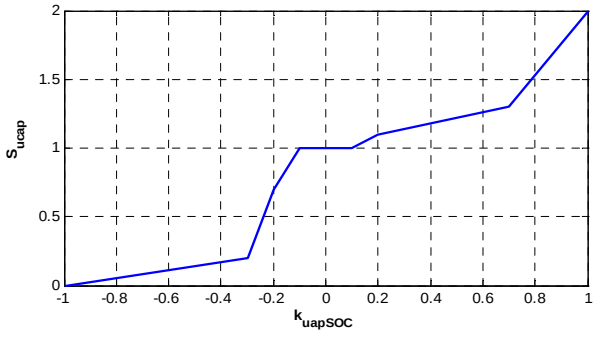

Fig. 9 S_{ucap} according to $k_{ucap.SOC}$

The power distribution between the ESS and the EGS is accomplished in the second step. In this step, the equivalence between electrical energy and fuel energy is evaluated by considering average energy converting efficiency. The power distribution among the EGS, the battery and the ultracapacitor is conducted by minimizing the instantaneous cost function. The instantaneous cost function including the EGS, the battery, and the ultracapacitor power is shown in equation (14).

$$\min_{P_{egs}} J_{total}(n) = \min_{P_{egs}} \{ \frac{1}{\eta_{egs}(P_{egs}(n))} P_{egs}(n) + E_{egs.change}(n) + \frac{S_{bat}}{\eta_{egs.ave}} P_{bat.in}(P_{bat}(n)) + \frac{S_{bat} S_{ucap}}{\eta_{egs.ave}} P_{ucap.in}(P_{ucap}(n)) \} \quad (14)$$

which is subjected to $P_{des} = P_{egs} + P_{ESS}$, $P_{bat} = u_1 \cdot P_{ESS}$, $P_{ucap} = P_{ESS} - P_{bat}$, $0 \le P_{egs} \le P_{egs.max}$.

The optimal power distribution can be obtained by varying the EGS demand power from 0 to $P_{egs.max}$ and selecting the power distribution at the minimum cost J_{total} because an one dimensional optimal map as a function of EGS demand power is obtained in the first step as shown in equation (14).

S_{bat} is a charge sustaining factor of the battery and is decided as shown in Fig. 10. If the battery SOC is high, S_{bat} has small value so that the battery tends to discharge. On the other hand, if the battery SOC is low, S_{bat} has large value to charge the battery.

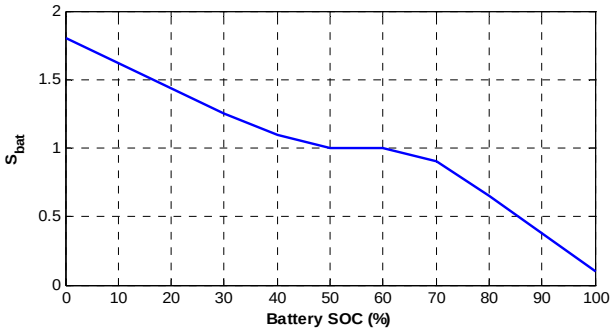

Fig. 10 S_{bat} according to battery SOC

The demand power of the battery is weighted according to the S_{bat} in order to sustain the battery SOC in an appropriate level.

In equation (14), $\eta_{egs.ave}$ is the average EGS efficiency for converting fuel energy to electrical energy and can be calculated as follows

$$\eta_{egs.ave} = \frac{1}{t} \int_0^t \eta_{egs}(P_{egs}(n))\, dn \quad (15)$$

The equivalence factor that converts the electrical energy into equivalent fuel energy is related to the average energy converting efficiency. In the case of the SHEV, an inverse of average EGS efficiency $1/\eta_{egs.ave}$ is an equivalence factor converting electrical energy to equivalent fuel energy because only the EGS is involved in the energy conversion process.

$E_{egs.change}$ is a variable to calculate the EGS operating point transition energy. Transition of the EGS operating point lead to a change of rotational kinetic energy of the EGS and it can cause additional energy consumption; therefore, $E_{egs.change}$ is added in the instantaneous cost function shown in equation (14) as a penalty. $E_{egs.change}$ represents additional consumed fuel energy to transit the operating point of the EGS in an actual vehicle. Suppose that this energy consumption occurred in a generator, the consumed energy is calculated by equation (16)

This article has been accepted for publication in a future issue of this journal, but has not been fully edited. Content may change prior to final publication. Citation information: DOI 10.1109/TVT.2015.2445872, IEEE Transactions on Vehicular Technology

$$E_{egs.change}(n) = \frac{I_{eng} \left\| \omega_{eng}(n)^2 - \omega_{eng}(n-1)^2 \right\|}{2 \times \eta_{gen.change}(n) \times \eta_{egs.ave}} \quad (16)$$

where $\eta_{gen.change}$ is efficiency of generator that is shown in equation (17).

$$\eta_{gen.change}(n) = \begin{cases} \eta_{gen}(P_{egs}(n)) & when,\ w(n) < \omega(n-1) \\ \eta_{gen}(P_{egs}(n-1)) & when,\ w(n) \geq \omega(n-1) \end{cases} \quad (17)$$

If the EGS accelerates (i.e., $\omega(n) \geq \omega(n-1)$), $E_{egs.change}$ is calculated using the efficiency at the current (i.e., at $n-1$) EGS operating point because the energy to accelerate the EGS inertia is consumed at the current operating point. On the other hand, If the EGS decelerates (i.e., $\omega(n) < \omega(n-1)$), the efficiency at the changed (i.e., at n) EGS operating point is used because the energy to accelerate the EGS inertia is consumed at the changed operating point.

IV. Simulation

A. Simulation Environment

The simulation was conducted to verify the accuracy and effectiveness of the proposed supervisory control algorithm. The simulation program consists of the SHEV model and the supervisory controller, as shown in Fig. 11. A vehicle powertrain model package, AVL CRUISE® which is widely used in fuel economy studies [28, 29, 30, 31] was used to construct the SHEV model and FTP-72 driving cycle shown in Fig. 12 is used as a velocity profile for the simulation.

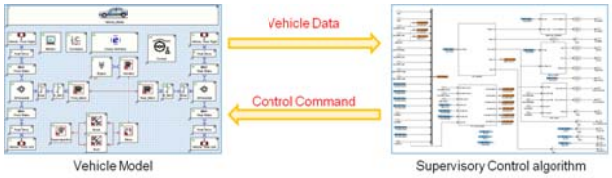

Fig. 11 Matlab/Simulink® – AVL Cruise® co-simulation environment

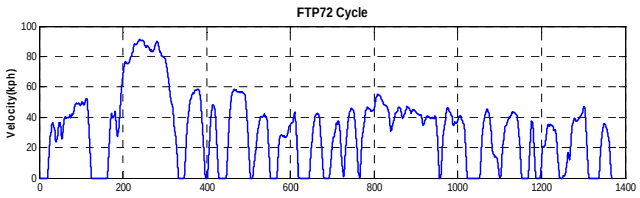

Fig. 12 FTP-72 drive cycle

B. Simulation Results

1) Optimal Torque Distribution

Fig. 13 to 15 show the comparison between the proposed optimal torque distribution and a uniform torque distribution. In figure 13, the electrical energy consumed by two traction motors during FTP-72 driving cycle is presented according to distribution strategies. As shown in Fig. 13, the consumed electrical energy of the optimal torque distribution is less than that of the uniform torque distribution. Fig. 14 and 15 show the operating points of two traction motors and Table V compares the average traction motor efficiencies of the optimal torque distribution strategy with those of the uniform torque distribution strategy. As shown in Fig. 15, the optimal torque distribution strategy forces the traction motors to operate at the operating points with high efficiency by considering the efficiency of two traction motors while the uniform torque distribution strategy distributes the traction torque uniformly to the front and rear motors regardless of an efficiency concern. Therefore, Table V shows that the average efficiency of the optimal torque distribution is better than that of the uniform torque distribution.

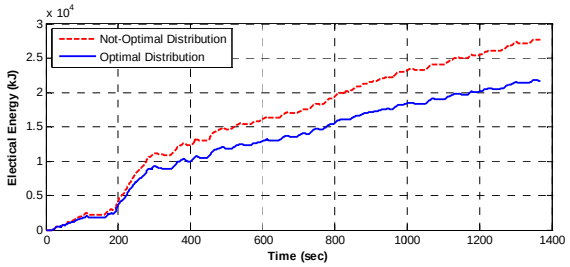

Fig. 13 Consumed electrical energy in two motors according to distribution strategies

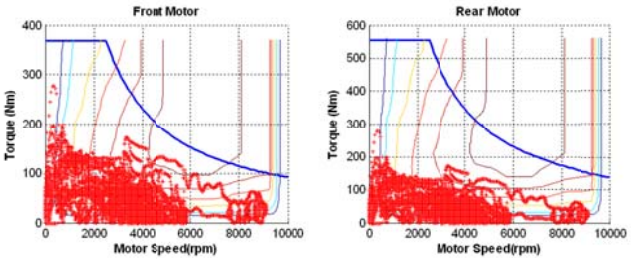

Fig. 14 Operating point of two motors in uniformly distribution

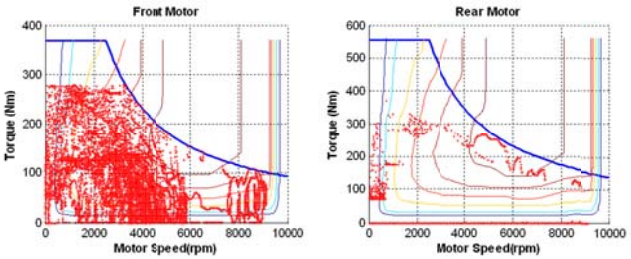

Fig. 15 Operating point of two motors in optimal distribution

2) Power Distribution

In this section, vehicle simulations by the TCS, the PCS, and the ECMS strategies are conducted and simulation results are compared between different strategies. Not only the fuel economy but also the efficiency of each component (the battery, the ultracapacitor, and the EGS) and the battery usage are compared. The battery usage is defined as shown in equation (18).

$$\text{Battery Usage} = \sqrt{\frac{1}{T_f}\int_0^{T_f} P_{bat.fnl}{}^2(t)\,dt} \quad (18)$$

Since initial and final SOCs of the battery and the ultracapacitor can be different, SOC differences must be compensated to compare fuel economies between different

This article has been accepted for publication in a future issue of this journal, but has not been fully edited. Content may change prior to final publication. Citation information: DOI 10.1109/TVT.2015.2445872, IEEE Transactions on Vehicular Technology

strategies. The energy compensation terms can be calculated with difference between first and final energy levels of the battery and the ultracapacitor. The energy level differences are calculated with SOCs, average voltages, and capacities of the battery and the ultracapacitor as given in equation (19) and (20).

$$\Delta E_{bat} = \frac{\Delta SOC_{bat}}{Battery\ \ total\ \ energy} = \frac{SOC_{bat.fnl} - SOC_{bat.ini}}{C_{bat} \times V_{bat.ave} \times 3600} \quad (19)$$

$$\Delta E_{ucap} = \frac{1}{2} C_{uacp} \left(V_{ucap.fnl}{}^2 - V_{ucap.ini}{}^2 \right) \quad (20)$$

The compensation energy provided to the battery and the ultracapacitor by the EGS is given in equation (21). If the compensation energy is assumed to be supplied by the EGS average power, the EGS operation time is calculated by equation (22). The compensation fuel can be calculated using the EGS operation time and the fuel consumption at the EGS operating point.

$$\Delta E_{i.comp} = \begin{cases} -\Delta E_i \times \eta_{i.ave} & when,\ \Delta E_i \geq 0 \\ -\Delta E_i / \eta_{i.ave} & when,\ \Delta E_i < 0 \end{cases} \quad i = bat,\ ucap \quad (21)$$

$$\Delta t_{comp} = \frac{\Delta E_{bat.comp} + \Delta E_{ucap.comp}}{P_{egs.ave}} \quad (22)$$

$$\Delta Fuel = SFC(T_{egs.ave}, w_{egs.ave}) \cdot P_{egs.ave} \cdot \frac{\Delta t_{comp}}{3600} \quad (23)$$

where $\eta_{i.ave}$ (i.e., $\eta_{bat.ave}$ and $\eta_{ucap.ave}$) is the average efficiency of the energy storages (i.e., battery and ultracapacitor). SFC in equation (23) is fuel consumption rate when EGS operates on the average power operating point. The total fuel economy including ESS energy compensation is represented in equation (24).

$$Fuel\ Economy = \frac{Driving\ \ Distance}{(Fuel + \Delta Fuel) \times Fuel\ Density} \quad (24)$$

Fig. 16 and 17 represent simulation results of the LPF based TCS strategy and the proposed TCS strategy, respectively. As seen in Fig. 16, ultracapacitor SOC decreases because the LPF strategy does not sustain ultracapacitor SOC. Thus, battery output power increases at low ultracapacitor SOC region because the ultracapacitor cannot supply enough demand power to the bus. On the other hand, the proposed TCS strategy (Fig. 17) can maintain ultracapacitor SOC and so battery output power can be maintained at the relatively steady value.

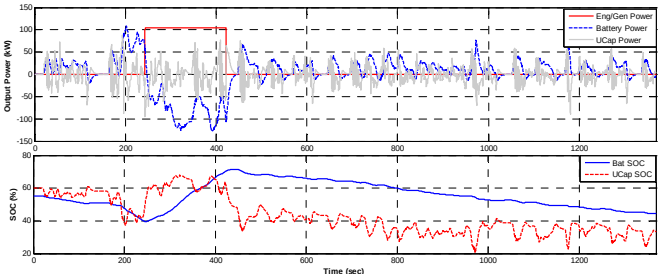

Fig. 16 Power distribution results of the LPF based TCS

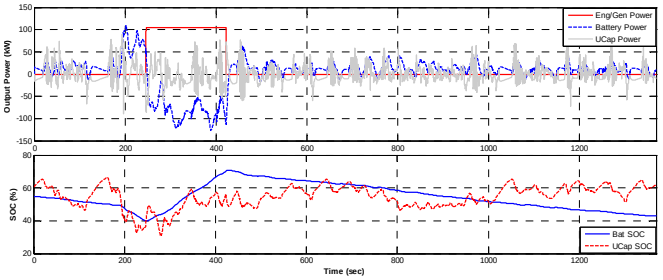

Fig. 17 Power distribution results of the proposed TCS

Fig. 18 and 19 represent simulation results of the LPF based PCS strategy and the proposed PCS strategy, respectively. Unlike the TCS strategies, the simulation results show that EGS output power is adjusted according to battery SOC. Consequently, battery SOC swing range by the PCS strategies is narrower. The differences between the LPF strategy and the proposed strategy of the PCS are similar to the TCS case.

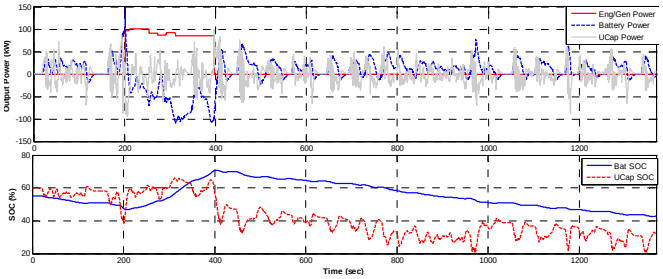

Fig. 18 Power distribution results of the LPF based PCS strategy

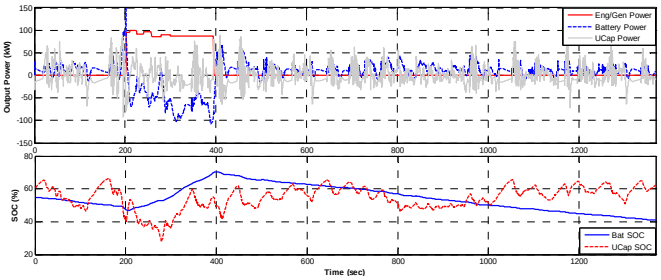

Fig. 19 Power distribution results of the proposed PCS strategy

Fig. 20 shows simulation results of the proposed ECMS. Unlike the TCS and the PCS cases, the ECMS decides the optimal EGS operation by minimizing the instantaneous cost function. Therefore, EGS operating points change more frequently and the swing range of battery SOC is narrower by the ECMS than by the other strategies.

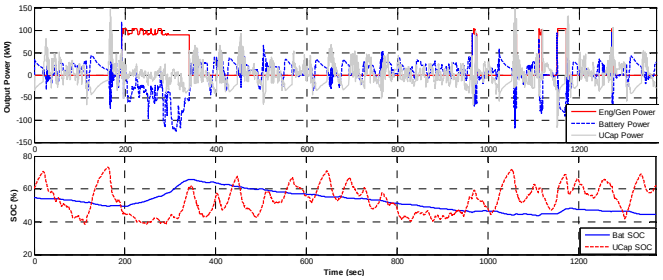

Fig. 20 Power distribution results of the proposed ECMS strategy

This article has been accepted for publication in a future issue of this journal, but has not been fully edited. Content may change prior to final publication. Citation information: DOI 10.1109/TVT.2015.2445872, IEEE Transactions on Vehicular Technology

Since, in this paper, the instantaneous cost function is defined to let the ultracapacitor work as a LPF for the battery and to manage ultracapacitor SOC based on vehicle velocity, power distribution of the ECMS between the battery and the ultracapacitor is similar to that of the proposed TCS and the proposed PCS.

To make sure that ultracapacitor SOC is managed based on vehicle speed, Fig.21 shows the relation between vehicle speed and ultracapacitor SOC. As shown in Fig. 21, ultracapacitor SOC increases as vehicle speed decreases; and ultracapacitor SOC increases by regeneration energy during the braking.

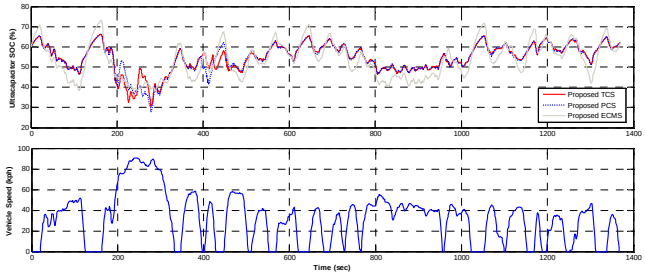

Fig. 21 Ultracapacitor SOC and vehicle speed

Fig. 22 to 24 represent specific fuel consumption (SFC) of the engine, OOL (red dashed line) of the EGS, and EGS operating points (cross marks) for each control strategy. As shown in figures, the EGS is operated at OOP by the TCS strategies while the EGS is operated at OOL by the other strategies. The EGS operating points located outside of OOP or OOL are the transient points between the EGS off state and target operating points decided by the given required power. As shown in Fig. 24, the transient points of the ECMS case are more scattered because the ECMS strategy requires more frequent on-off of the EGS.

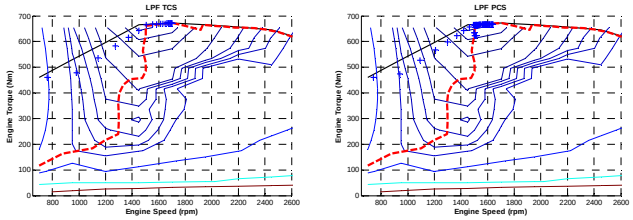

Fig. 22 Engine/Generator operating points by the LPF based TCS/PCS

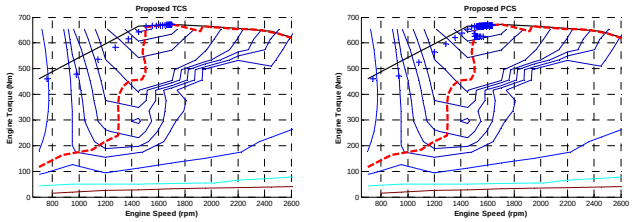

Fig. 23 Engine/Generator operating points by the proposed TCS/PCS

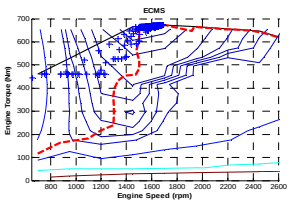

Fig. 24 Engine/Generator operating points by the proposed ECMS strategy

Table VI shows summary of simulation results with FTP-72 speed profile. It includes fuel economy increments compared to the same class conventional military vehicle whose fuel economy is 5.6 km/L. The ECMS delivers the best fuel economy increment while the TCS and the PCS strategies with LPF provide the lowest results.

The TCS strategies cause lower battery efficiency than the PCS strategies because of wider SOC swing range. Therefore, even though the TCS strategies provide better EGS efficiency, these strategies show lower fuel economy than the PCS strategies due to lower battery and ultracapacitor efficiencies. The proposed strategies for both the TCS and the PCS offer better fuel economy than the LPF strategies because the proposed strategies let the ultracapacitor operate at high efficiency region by sustaining ultracapacitor SOC.

The ultracapacitor cannot operate as a LPF for battery in the low ultracapacitor SOC region. Therefore, since LPF strategies cannot properly manage the ultracapacitor SOC in the low ultracapacitor SOC region, the battery demand power increases. However, since the proposed strategies have a function that keeps the ultracapacitor SOC at a certain level, the proposed strategies can let the ultracapacitor keep acting as a LPF and lower battery usage.

Since the ECMS is designed to optimize the fuel economy, fuel economy is improved because average efficiency of the EGS is increased remarkably and so fuel economy is improved, even though battery usage increases and battery efficiency decreases.

TABLE VI
FTP-72 DRIVE CYCLE SIMULATION RESULTS SUMMARY

	Fuel Economy (km/L)	Battery Eff. (%)	Ucap. Eff. (%)	Engine Eff. (%)	Battery Usage (kW)
LPF TCS	6.2665 (11.9%)	96.44	95.57	37.34	1.0512
Proposed TCS	6.3912 (14.1%)	96.66	97.66	37.34	0.9927
LPF PCS	6.294 (12.4%)	97.18	96.04	36.96	0.8533
Proposed PCS	6.4429 (15.1%)	97.46	97.69	36.98	0.7831
ECMS	6.683 (19.3%)	97.44	97.54	37.11	0.805

V. CONCLUSION

In this paper, Supervisory control algorithms have been developed for optimal operation of the SHEV with multiple energy sources.

The main contributions of this paper are listed as follows:

- The optimal torque distribution strategy calculates the optimal torque distribution ratio between front and rear motor using the motor efficiency map.
- The TCS and the PCS are modified to improve fuel efficiency and maintain ultracapacitor SOC within a certain boundary for the SHEV with multiple energy storages.
- A new ECMS is proposed and designed with a power distribution strategy between battery and ultracapacitor of the SHEV.

The SHEV model (simulation program) is designed using AVL CRUISE® to show the effectiveness of control strategies.

This article has been accepted for publication in a future issue of this journal, but has not been fully edited. Content may change prior to final publication. Citation information: DOI 10.1109/TVT.2015.2445872, IEEE Transactions on Vehicular Technology

Simulation results show that the optimal torque distribution strategy improves average front and rear motor efficiencies up to 8.41% for the front motor and 3.99% for the rear motor. The proposed TCS and PCS strategies show improvements on three aspects; they reduce the abrupt battery power changes, improve the fuel economy, and maintain ultracapacitor SOC within a certain level. An ECMS is also proposed for the SHEV with multiple energy storages to improve fuel efficiency and to maintain SOC. The cost function of the ECMS includes change rate of the battery power and the EGS operating point transition energy. Simulation results show that the ECMS provides the best performance in terms of fuel efficiency and maintainability of ESS SOC within a certain boundary.

REFERENCES

[1] M. Gokasan, S. Bogosyan and D. J. Goering, "Sliding Mode Based Powertrain Control for Efficiency Improvement in Series Hybrid-Electric Vehicles", *IEEE Trans. Power Electron.*, vol. 21, no. 3, pp. 779-790, May. 2006.

[2] C. G. Hochgraf, M. J. Ryan and H. L. Wiegman, "Engine control Strategy for a Series Hybrid Electric Vehicle Incorporating Load-Leveling and Computer Controlled Energy Management", *SAE technical paper 960230*, pp.1-14, Feb. 1996.

[3] C. Liang, W. Weihua and W. Qingnian, "Energy Management Strategy and Parametric Design for Hybrid Electric Military Vehicle", *SAE Technical Paper 2003-01-0086,* pp.1-6, Mar. 2003.

[4] Y. Gao and M. Ehsani, "Parametric Design of the Traction Motor and Energy Storage for Series Hybrid Off-Road and Military Vehicles", *IEEE Trans. Power Electron.*, vol. 21, no. 3, pp. 749-755, May. 2006.

[5] G. Khalil, "Challenges of Hybrid Electric Vehicles for Military Applications", in *Proc. IEEE Veh. Power Propulsion Conf.,* 2009, pp.1-3

[6] A. Sciarretta and L. Guzzella, "Control of hybrid electric vehicles", *IEEE Control Systems Mag.*, pp. 60-70, Apr. 2007.

[7] P. Pisu and G. Rizzoni, "A Comparative Study of Supervisory Control Strategies for Hybrid Electric Vehicles", *IEEE Trans. Control Syst. Technol.*, vol. 15, no. 3, May. 2007.

[8] F. R. Salmasi, "Control strategies for hybrid electric vehicles: evolution, classification, comparison, and future trends," *IEEE Trans. on Veh. Technol*, vol.56, no.5, pp. 2393 -2404, Sep. 2007.

[9] N. Jalil, N. A. Kheir, and M. Salman, "A rule-based energy management strategy for a series hybrid vehicle", in *Proc. Amer. Control Conf.,* 1997*,* pp 689-693.

[10] C. Shu-mei, T. De-wen, and Z. Qian-fan, "Study of Hybrid Energy Control Strategy for Hybrid Electric Drive System in All Electric Combat Vehicles", in *Proc. IEEE Veh. Power Propulsion Conf.,* 2008, pp. 1-5.

[11] M. Ehsani, Y. Gao, S. E. Gay, and A. Emadi, "Modern Electric, Hybrid Electric, and Fuel Cell Vehicles: Fundamentals, Theory, and Design" Boca Raton, FL: CRC, 2004.

[12] L. Chu, Q. Wang, M. Liu and J. Li, "Development and Validation of Control Algorithm for Series Hybrid Power Train", *SAE Technical Paper* 2003-01-3281, pp.1-7, Oct. 2003.

[13] J. Gao, F. Sun, H. He, G. G. Zhu and E. G. Strangas, "A Comparative Study of Supervisory Control Strategies for a Series Hybrid Electric Vehicle", in *Proc. Power and Energy Engineering Conf.*, 2009, pp. 1-7.

[14] A. C. Baisden and A. Emadi, "ADVISOR-Based Model of a Battery and an Ultra-Capacitor Energy Source for Hybrid Electric Vehicles", *IEEE Trans. Veh. Technol.*, vol. 53, no.1, pp.199-205, Jan. 2004.

[15] S.G. Li, S.M. Sharkh, F.C. Walsh, and C.N. Zhang, "Energy and Battery Management of a Plug-In Series Hybrid Electric Vehicle Using Fuzzy Logic", *IEEE Trans. Veh. Technol.*, vol. 60, no.8, Oct. 2011.

[16] W. Shabbir, C. Arana, S. A. Evangelou, "Series Hybrid Electric Vehicle Supervisory Control Based on Off-line Efficiency Optimization", in *Proc. IEEE International Electric Vehicle Conference (IEVC),* 2012, pp. 1-5.

[17] B. Lu, B. Natarajan, N. Schulz, "Optimal Control based Power Management in Hybrid Military Vehicle", in *Proc. IEEE International Electric Vehicle Conference (IEVC),* 2012, pp. 1-7.

[18] A. A. Malikopoulos, "Stochastic Optimal Control for Series Hybrid Electric Vehicles", in *Proc. Amer. Control Conf.*, 2012, pp. 1189-1194.

[19] S. Barsali, C. Miulli and A. Possenti, "A Control Strategy to Minimize Fuel Consumption of Series Hybrid Electric Vehicles", *IEEE Trans. Energy Conversion*, vol. 19, no. 1, pp.187-195, Mar. 2004.

[20] J-P Gao, G-M G Zhu, E G Strangas, and F-C Sun, "Equivalent fuel consumption optimal control of a series hybrid electric vehicle", *Proc. IMechE,* vol. 223 Part D: J. Automobile Engineering, pp.1003-1018, Apr. 2009.

[21] A. F. Burke, "Batteries and Ultracapacitors for Electric, Hybrid, and Fuel Cell Vehicles", in *Proc. of the IEEE*, vol.95, no.4, pp.806-820, Apr. 2007.

[22] Y. Ko, H. Kim, Y. Jung, S. Jeong, H. Choi, Y. Lee, and H. Lee, "Powertrain Equipments size selection of Series Hybrid Vehicle", in *Proc. KSAE,* 2009, pp.2943-2952. (Korean)

[23] L. Serrao, S. Onori and G. Rizzoni, "ECMS as a realization of Pontryagin's minimum principle for HEV control", in *Proc. Amer. Control Conf.*, 2009, pp.3964-3969.

[24] V. Sezer, M. Gokasan, S. Bogosyan, "A Novel ECMS and Combined Cost Map Approach for High-Efficiency Series Hybrid Electric Vehicles, *IEEE Trans. Veh. Technol.*, vol. 60, no. 8, pp.3557-3570, Oct. 2011.

[25] R. Razavian, N. L. Azad, J. McPhee, "On Real-Time Optimal Control of A Series Hybrid Electric Vehicle with an Ultra-Capacitor", in *Proc. Amer. Control Conf.*, 2012, pp.547-552.

[26] S. Burch, M. Cuddy, and T. Markel, ADVISOR 2002 Documentation. Nat. Renewable Energy Lab., 2002.

[27] Y. Jung, H. Kim, Y. Ko, S. Jeong, H. Choi, Y. Lee and H. Lee, "Power Distribution Strategy for a Series Hybrid Electric Vehicle Consisting of Engine/Genernтor, Battery and Ultra-capacitor", in *Proc. KSAE,* 2010, pp. 1755-1759. (Korean)

[28] L. Wang, Y. Zhang, C. Yin, M. Zhang, "Design and Simulation for a Series-parallel Hybrid Electric City-bus", in *Proc. IEEE Veh. Power Propulsion Conf.,* 2009, pp. 1767-1772.

[29] B. Zhang, G. Xu and L. Fang, "Study on Control Strategy and Simulation for ISG_Type Parallel Hybrid Electric Vehicle", *Advanced Control of Industrial Processes (ADCONIP),* 2011, pp.498-502.

[30] Y. Peng, M. Shang, X. Zeng, D. Song, Q. Zhu, G. Bai, C. Zhang, "Control Strategy of Four-Wheel Drive Plug-in Hybrid Electric Vehicle", *Instrumentation and Measurement, Sensor Network and Automaton (IMSNA),* 2013, pp.532-535.

[31] X. Zeng, Y. Peng, D. Song, "Powertrain Parameter Matching of A Plug-In Hybrid Electric Vehicle", *Transportation Electrification Asia-Pacific (ITEC Asia-Pacific),* 2014, pp.1-5.

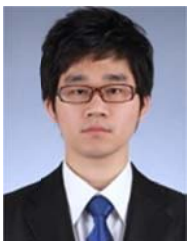

Youngkwan Ko received the B.S. degree in mechanical engineering and M.S. degree in electric engineering from Hanyang university, Seoul, Korea in 2009 and 2011, respectively. Since 2011.

He is currently researching a motor controller to suppress the drive-line vibration of hybrid electric vehicles and electric vehicles with Hyundai-Kia Motors Group R&D center.

Jeeho Lee received the B.S. degree in electrical engineering from Hanyang University, Seoul, Korea, in 2007, where he is currently working toward the Ph.D. degree. His current research interests are hybrid power train control, energy storage hybridization, and applications to vehicle control.

Hyeongcheol Lee (M'10) received the B.S. and M.S. degrees from Seoul National University, Seoul, Korea, in 1988 and 1990, respectively, and the Ph.D. degree from the University of California at Berkeley, in 1997. Currently, he is a Professor with the Division of Electrical and Biomedical Engineering of Hanyang University, Seoul, Korea. His research interests include adaptive and nonlinear control, embedded systems, applications to vehicle controls, and vehicle dynamics.